Alleles of *afd1* dissect REC8 functions during meiotic prophase I

Inna N. Golubovskaya[1,2,*], Olivier Hamant[1,*], Ljuda Timofejeva[3], Chung-Ju Rachel Wang[1], David Braun[4,‡], Robert Meeley[5] and W. Zacheus Cande[1,§]

[1]Department of Molecular and Cell Biology, University California, Berkeley, CA 94720, USA
[2]N. I. Vavilov Institute of Plant Breeding, St Petersburg, 190000, Russia
[3]Department of Gene Technology, Tallinn University of Technology, 19086, Estonia
[4]Department of Plant and Microbial Biology, University California, Berkeley, CA 94720, USA
[5]Pioneer Hi-Bred International, 7300 NW 62nd Ave, Johnston, IA 50131-1004, USA

*These authors contributed equally to this work
‡Present address: Department of Biology, 208 Mueller Lab, Pennsylvania State University, PA 16802, USA
§Author for correspondence (e-mail: zcande@uclink4.berkeley.edu)

Accepted 17 May 2006
Journal of Cell Science 119, 3306-3315 Published by The Company of Biologists 2006
doi:10.1242/jcs.03054

Summary

REC8 is a master regulator of chromatin structure and function during meiosis. Here, we dissected the functions of *absence of first division* (*afd1*), a maize *rec8/α-kleisin* homolog, using a unique *afd1* allelic series. The first observable defect in *afd1* mutants is the inability to make a leptotene chromosome. AFD1 protein is required for elongation of axial elements but not for their initial recruitment, thus showing that AFD1 acts downstream of ASY1/HOP1. AFD1 is associated with the axial and later the lateral elements of the synaptonemal complex. Rescuing 50% of axial element elongation in the weakest *afd1* allele restored bouquet formation demonstrating that extent of telomere clustering depends on axial element elongation. However, rescuing bouquet formation was not sufficient for either proper RAD51 distribution or homologous pairing. It provides the basis for a model in which AFD1/REC8 controls homologous pairing through its role in axial element elongation and the subsequent distribution of the recombination machinery independent of bouquet formation.

Supplementary material available online at
http://jcs.biologists.org/cgi/content/full/119/16/3306/DC1

Key words: Meiosis, REC8, Leptotene chromosome, Axial element, RAD51, Bouquet

Introduction

Meiotic prophase is initiated by the formation of a unique and cytologically characteristic leptotene chromosome. The establishment of leptotene chromosome structure relies, at least partly, on the installation of proteinaceous axial elements (AEs) onto the chromosomes. Once leptotene chromosome structure is established, several unique meiotic events occur, including telomeres attaching to the inner nuclear envelope, telomere clustering into a bouquet and recruitment of the recombination machinery. This is followed by homologous pairing and synapsis. As the chromosomes zip up during synapsis, a central element is installed between the AEs (now called lateral elements) of the two homologous chromosomes, completing the formation of the synaptonemal complex (SC). Recombination is probably initiated in leptotene, and some recombination events mature in crossovers during synapsis, yielding chiasmata that, in conjunction with sister chromatid cohesion (SCC), hold maternal and paternal chromosomes together until the transition from metaphase I to anaphase I. Sister chromatids segregate to daughter nuclei during meiosis II. This two-step chromosome segregation relies on a sequential dissociation of SCC.

In meiosis, sister chromatids are held together through the first meiotic division, and rely on meiosis-specific SCC components. In yeast, REC8, a member of the α-kleisin superfamily of SMC protein partners (Schleiffer et al., 2003), is a key component of the cohesion complex and is absolutely required for chromosome segregation during meiosis (Watanabe and Nurse, 1999). Mutations in *rec8* have been identified and characterized in a number of organisms including *Saccharomyces cerevisiae*, *Schizosaccharomyces pombe*, *Caenorhabditis elegans*, *Arabidopsis thaliana* and mouse, and their analysis has shown that the role of REC8 in cohesion is conserved across kingdoms (Uhlmann, 2003; Lee and Orr-Weaver, 2001; Nasmyth, 1999; Kitajima et al., 2003; Stoop-Myer and Amon, 1999; Page and Hawley, 2003). Furthermore, the analysis of *rec8* mutant phenotypes revealed additional REC8 functions in leptotene chromosome structure, AE formation, homologous pairing, synapsis and recombination. However depending on the organism, the *rec8* phenotypes are variable and the exact role of REC8 in all these events is controversial (Lin et al., 1992; Molnar et al., 1995; Bai et al., 1999; Bhatt et al., 1999; Klein et al., 1999; Watanabe and Nurse, 1999; Pasierbek et al., 2001; Chelysheva et al., 2005; Xu et al., 2005). In particular, the link between REC8 and synapsis is under debate. Although AE formation is impaired in *rec8* mutants from most organisms studied, cytologically wild-type synaptonemal complexes (SCs) form in mouse *rec8* mutants, suggesting that REC8 is not required for AE formation in mammals (Xu et al., 2005). The role of REC8 in homology recognition is also poorly understood. Characterization of *rec8* mutants has shown that, depending on

the organism, homologous recognition either does not occur at all (yeast, *Arabidopsis*), is initiated but is not completed (*C. elegans*) or occurs between sister chromatids rather than homologs (mouse) (Bai et al., 1999; Cai et al., 2003; Pasierbek et al., 2001; Xu et al., 2005).

One way to deepen our knowledge of REC8 functions is to study the phenotypic effects of an allelic series of this gene. Very few *rec8* mutant alleles have been isolated, and monitoring chromosome structure in yeast, the best-documented model organism for REC8 functions, remains difficult owing to the small size of its chromosomes. Here, we report the cloning of *absence of first division* (*afd1*; GenBank accession number AY788900) in maize, and show that it encodes an α-kleisin homolog. Based on its sequence similarity to the rice and *Arabidopsis rec8* gene, and its meiosis-specific function, we call *afd1* a *rec8* homolog. This is the first report of the cloning of a *rec8/α-kleisin* homolog in maize. In this study, we focused on the role of AFD1 during early prophase I. Based on the phenotype of the null-alleles, we show that AFD1 is required for establishing leptotene chromosome structure, bouquet formation, pairing and synapsis as already shown in other *rec8* mutants. Our unique series of weaker *afd1* alleles shows a range of defects in prophase I events, allowing us to investigate for the first time the role of AFD1/REC8 in the coordination of these events. We showed that AFD1 is not required for AEs initial recruitment but instead is controlling the extent of AEs elongation and their maturation into lateral elements during synapsis. Surprisingly, partial AEs elongation was sufficient for leptotene chromosome structure establishment and bouquet formation. By contrast, homologous pairing, synapsis and proper distribution of RAD51 depended on full AEs elongation, providing the basis for a model in which AFD1 controls homologous pairing through its role in AEs elongation and the subsequent distribution of the recombination machinery independent of bouquet formation.

Results

afd1 encodes a REC8 homolog

In a directed *Mutator* (*Mu*)-tagging experiment for a very closely linked gene, *tdy1*, we obtained a new *afd1* allele, *afd1-2*, that had a large deletion encompassing part of the *afd1* gene. Sequencing analysis of one of the regions flanking the deletion in *afd1-2* uncovered a truncated open reading frame (ORF) with close identity to the 5′ sequence of *rec8*. We obtained two additional insertion lines in this *rec8* homolog, named *afd1-3* and *afd1-4*, by reverse genetics in the trait utility system for corn (TUSC) transposon mutagenesis program at Pioneer Hi-Bred (Meeley and Briggs, 1995; Chuck et al., 1998). Sequencing the alleles revealed that *afd1-1* contains a G to A alteration at the 5′ splice site of intron 16, introducing a premature stop codon and leading to a truncated protein lacking 141 C-terminal amino acids (Fig. 1A). A *Mu* insertion occurred 40 bp downstream of the donor site of intron 3 in *afd1-3*, and 80 bp downstream of the donor site of intron 1 in *afd1-4* (Fig. 1B). All three new *afd1* alleles were sterile and displayed comparable phenotypes to *afd1-1* after anaphase I (Golubovskaya and Mashnenkov, 1975) (see below). Based on these results and an allelism test between all the *afd1* alleles (see Materials and Methods), we concluded that we cloned the *afd1* gene.

By using reverse transcriptase (RT) and rapid amplification of cDNA ends (RACE)-PCR we isolated a 2300 bp long full-length *afd1* cDNA encoding a predicted protein of 602 amino acids. The *afd1* gene is complex: it contains 20 exons and 19 introns. Although AFD1 displays a stronger sequence identity with mammalian RAD21 than mammalian REC8, AFD1 exhibits the highest sequence identity (39%) with the *Arabidopsis* REC8 ortholog SYN1, and a weaker sequence identity with the three *Arabidopsis* RAD21 (Bai et al., 1999; Bhatt et al., 1999; Cai et al., 2003). In yeast, RAD21 functions in mitotic cohesion, and REC8 functions specifically in meiotic cohesion. In other organisms with multiple *α-kleisin/rad21/rec8* homologs, genes have been called *rec8* based on sequence and meiosis-specific function. AFD1 has the typical REC8/RAD21 N-terminal and C-terminal domains and possesses four putative separase cleavage sites, based on the (D/E)xxR consensus sequence described by Cai et al. (Cai et al., 2003) as well as several other putative protein binding sites (data not shown).

By RT-PCR, we showed that the *afd1* gene is expressed in leaves, tassel and ear, and to a lesser extent in roots and very young leaves of maize (Fig. 1C). *afd1* expression is thus not meiosis-specific, although the mutant phenotype is limited to reproductive organs. By RT-PCR, we did not detect any *afd1* transcripts in deletion allele *afd1-2,* as expected (Fig. 1D). Sequencing of *afd1* cDNA in *afd1-3* and *afd1-4* did not reveal any alteration in the *afd1* sequence. However, we detected lower levels of *afd1* expression in these two mutants as estimated by semi-quantitative RT-PCR (Fig. 1D,E).

afd1-3 and *afd1-4* are weak alleles

To check whether the AFD1 protein is expressed in *afd1-3* and *afd1-4*, we generated an AFD1-specific antibody and performed immunocytochemistry during pachytene. In the wild type, a bright signal was detected between homologous chromosomes and this pattern was very similar to that of SYN1/AtREC8 in *Arabidopsis* (Cai et al., 2003) (Fig. 1F). In the deletion allele *afd1-2*, no staining was detected in the nucleus (Fig. 1F). In *afd1-1*, no staining was detected in the nucleus, suggesting that the protein is either degraded or not properly localized because of the truncation in the protein sequence (Fig. 1F). By contrast, we detected a signal in the nuclei of *afd1-3* and *afd1-4* mutants. In *afd1-3*, based on the distribution of antibody staining only, we could not recognize individual chromosomes, although we detected 2 to 5 patches of staining per nucleus (Fig. 1F, arrowheads). In *afd1-4*, the AFD1 signal colocalized with the chromosomes, but was diffuse and faint compared to the wild type (Fig. 1F). When using an antibody raised against SYN1, the *Arabidopsis* homolog of AFD1, we obtained a similar but less distinct staining pattern in the four *afd1* alleles, confirming that the AFD1 staining truly correlates with the presence of AFD1 in the nucleus (supplementary material Fig. S1) (Cai et al., 2003). Altogether, these results showed that *afd1-2*, like most probably *afd1-1*, is a null-allele, whereas *afd1-3* and *afd1-4* are two weaker alleles of *afd1*.

AFD1 is a component of the axial elements

In wild-type zygotene, based on the AFD1 immunostaining only, we could recognize synapsed and unsynapsed

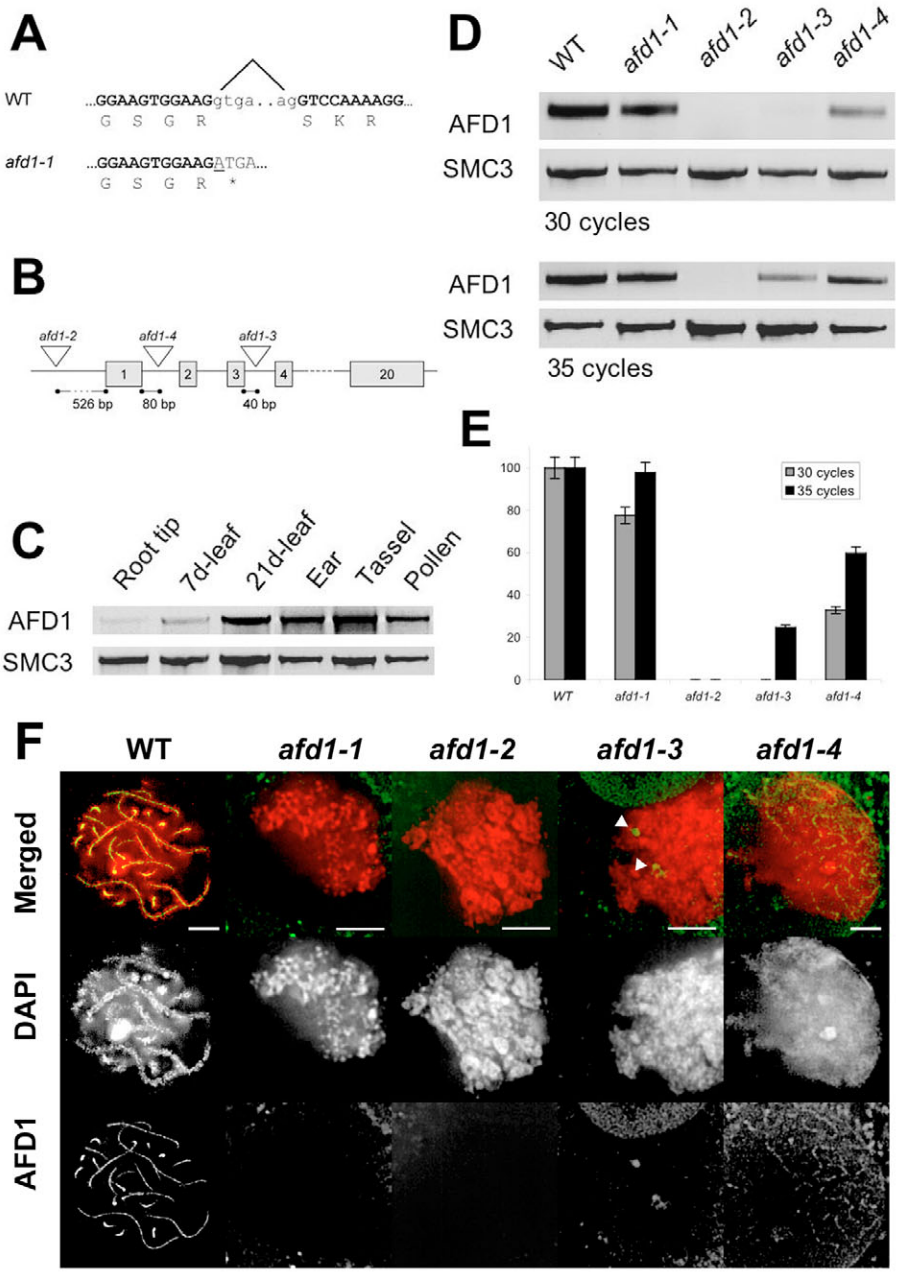

Fig. 1. *afd1* encodes a REC8 homolog. (A) Partial sequence of AFD1 in the wild-type and *afd1-1* mutant. In *afd1-1*, a G to A point mutation in the donor site of intron 16 (^) introduces a stop codon (*). (B) Position of the Mu insertions in *afd1-2*, *afd1-3* and *afd1-4*. (C) RT-PCR analysis of the *afd1* gene compared with *smc3* of root tips, leaves from 7-day-old and 21-day-old plants, ear at meiosis stage, tassel at meiosis stage, old-tassel-containing pollen. (D) RT-PCR analysis of the *afd1* gene compared with *smc3* in the tassel from wild-type and *afd1* alleles for 30 and 35 PCR cycles. (E) Quantification of the RT-PCR signal shown in D as a percentage of the wild-type signal intensity. (F) AFD1 immunolocalization (green in merged) in wild-type and *afd1* meiocytes stained with DAPI (red). Individual channels are shown in black and white for clarity. In the wild type, we observed a strong AFD1 signal between paired homologous chromosomes. In *afd1* mutants, we enhanced the signal to detect any signal on the chromosomes, thereby increasing the background signal. No staining was detected on the *afd1-1* and *afd1-2* chromosomes. In *afd1-3*, patchy signals were detected in the nucleus (arrowheads). In *afd1-4*, the AFD1 signal was diffuse and lines could be detected suggesting preferential colocalization with chromosomes. Bars, 5 μm.

chromosome regions (Fig. 2A). To further investigate the localization of AFD1 during prophase I in the wild type, we performed a double immunostaining with the AFD1 antibody and an antibody raised against ASY1/HOP1 (Armstrong et al., 2002). HOP1 is a structural component of the axial element (Hollingsworth et al., 1990; Smith and Roeder, 1997). ASY1/HOP1 and AFD1 signals colocalized at leptotene and zygotene, demonstrating that AFD1 contributes to the AEs. In synapsed regions, however, the ASY1/HOP1 signal became much dimmer and the AFD1 signal was brighter than it was in unsynapsed regions (Fig. 2B; supplementary material Fig. S2). Interestingly, in meiocytes fixed with 2% (instead of 4%) formaldehyde ASY1/HOP1 as well as AFD1 staining persisted through pachytene and appeared to be double-stranded with both proteins present on each strand (Fig. 2C). Visualization of two separate lateral elements and the persistence of ASY1/HOP1 staining might be due to a less compact chromatin structure and improved epitope accessibility of material fixed in 2% formaldehyde. The ASY1/HOP1 signal observed in meiocytes fixed in 4% formaldehyde is similar to that of PAIR2, the recently characterized rice homolog of HOP1, which was not clearly detectable between synapsed chromosomes (Nonomura et al., 2006). However, in meiocytes fixed in 2% formaldehyde, the ASY1/HOP1 signal is similar to that observed in *Arabidopsis* (Armstrong et al., 2002). To conclude, kinetics and pattern of the AFD1 signal as well as its colocalization with ASY1/HOP1 strongly suggest that AFD1 and ASY/HOP1 are components of both axial and lateral elements of SCs.

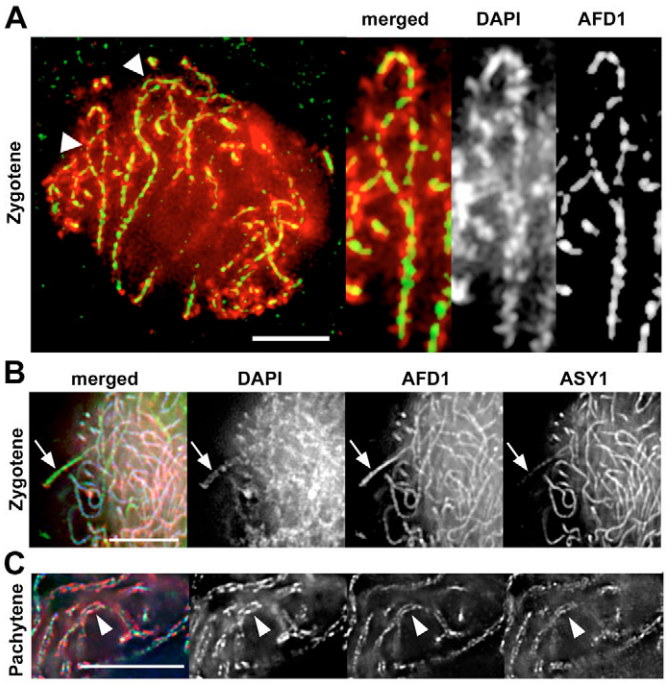

Fig. 2. AFD1 localizes to the axial and lateral elements. (A) Localization of AFD1 in a wild-type nucleus stained with DAPI (red) and anti-AFD1 antibody (green) at zygotene, showing an AFD1 signal on both synapsed and unsynapsed chromosome regions. Arrowheads indicate unsynapsed regions. The three panels on the right are magnifications of one region. Individual channels are shown in black and white for clarity. (B,C) Localization of AFD1 and ASY1/HOP1 in wild-type nuclei stained with DAPI (red), anti-AFD1 (green), and anti-ASY1/HOP1 antibodies (blue). Individual channels are shown in black and white for clarity. A projection view of a zygotene nucleus (4% paraformaldehyde fixation) is shown in B. AFD1 and ASY1/HOP1 signals are equally bright on unsynapsed chromosome regions. The ASY1/HOP1 signal is much dimmer where chromosomes are synapsed (arrow). (C) A projection view of a 0.4-μm section of the pachytene nucleus (2% paraformaldehyde fixation). AFD1 and ASY1/HOP1 colocalize and occur in between synapsed homologous chromosomes as two strands, marking the lateral elements. This pattern of immunostaining resembles silver-nitrate staining of lateral elements in SCs. Bars, 5 μm.

Prophase I chromosome structure is differently altered in the *afd1* alleles

To determine whether any of the defects present in nuclei from *afd1* null-alleles are partly rescued in the weaker *afd1* alleles, we first examined DAPI-stained nuclei during early prophase I in the four *afd1* alleles using 3D deconvolution light microscopy. Previously described criteria (Dawe et al., 1994; Bass et al., 1997; Golubovskaya et al., 2002) were used for accurate staging of the prophase I wild-type and *afd1*-mutant nuclei. From leptotene to zygotene in wild-type nuclei, the nucleolus moves to an off-center position and chromosomes form a crescent surrounding it (Fig. 3). Similar nucleolus behavior was observed in the four *afd1* alleles, thus facilitating the staging in these nuclei (Fig. 3). In wild type, leptotene chromosomes are organized as thin threads (Fig. 3A). At zygotene, whole-length chromosome threads are observed and telomeres cluster on the nuclear envelope (Fig. 3E). At pachytene, homologous chromosomes are aligned (Fig. 3I) and the installation of the SC is complete. Structural defects of meiotic chromosomes in *afd1-2* were similar to the ones observed in *afd1-1*: although leptotene, zygotene and pachytene stages could be identified based on nucleolus behavior and cell-shape and -size, chromosome morphologies could not be distinguished from each other because chromosomes formed a variable and fuzzy mass (Fig. 3B,F,J). By contrast, leptotene chromosome morphology was identified in both *afd1-3* and *afd1-4* mutants (Fig. 3C,D). In *afd1-4* but not in *afd1-3* the zygotene chromosome structure looked similar to that of wild type (Fig. 3G,H). As nuclei entered the stage corresponding to pachytene, chromosome morphology deteriorated in both weak alleles and was similar to that observed in *afd1-1* and *afd1-2* nuclei (Fig. 3K,L). Based on these data, we concluded that the absence of leptotene chromosome structure in the *afd1* null-allele could be rescued in weaker *afd1* alleles, strongly suggesting that AE elongation can occur in the weak *afd1* alleles.

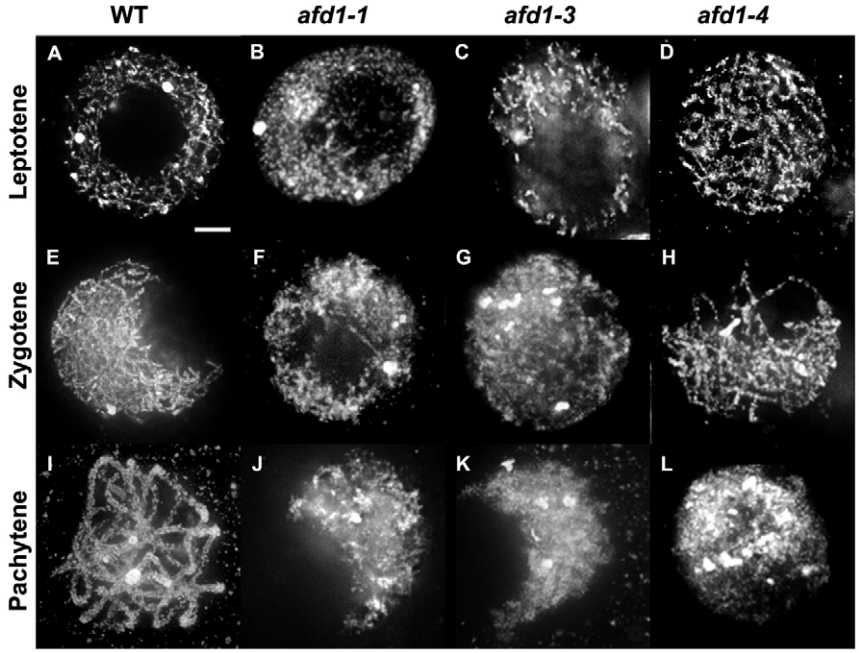

Fig. 3. Leptotene chromosome structure is rescued in weak *afd1* alleles. Wild-type and *afd1* nuclei stained with DAPI at leptotene (A-D), zygotene (E-H) and pachytene (I-L). Note the presence of chromosome threads at leptotene in the wild type, *afd1-3* and *afd1-4*, and their absence in *afd1-1*. Bar, 5 μm.

Axial elements recruitment occurs in all the *afd1* alleles, but their elongation is differently altered in the *afd1* alleles

To investigate the role of AFD1 in AE recruitment and elongation, we used transmission electron microscopy (TEM) of prophase I nuclei spreads (see Materials and Methods). This technique allowed us to identify proteinaceous structures and in particular AEs, based on their width and linear shape. To confirm the TEM data, we also performed immunostaining experiments with ASY1/HOP1, a component of the AEs (Hollingsworth et al., 1990; Smith and Roeder, 1997; Armstrong et al., 2002).

In the wild type, at pachytene, TEM micrographs show ten distinct SCs, each of them exhibiting two lateral elements that surround a central element (Fig. 4A,F). Although we never detected a normal SC in *afd1-1* and *afd1-2*, some AEs aggregates were observed in *afd1-1* and *afd1-2* (13.6±4.7 and 11.8±3.8 AEs aggregates per nucleus, respectively), showing that although AFD1 is required for normal AEs, it is not required for the initial recruitment of AEs (Fig. 4B,C). Although some linear shapes were observed in the AEs aggregates, they were shorter, often multilayered and the central element was never detected (Fig. 4G,H). This phenotype suggests that AFD1 is required for AE elongation and central element recruitment. In *afd1-3*, the number of synaptic structures slightly increased (18.9±4.5) and we also observed long stretches of 'shaggy' AEs forming a 'cobweb' around them, suggesting that AE elongation is partly rescued in *afd1-3* (Fig. 4D,I). In *afd1-4*, long AEs were recruited on chromosomes (Fig. 4E,J). The total length of AEs per nucleus ranged from 20-52% of that of wild type; and six of the 30 nuclei examined, were closer to the 52% upper limit. This is consistent with the fact that, in light-microscopy images, zygotene chromosome structure in this allele resembles that of the wild type. This further confirmed that AE elongation was partially rescued in a weak *afd1* allele. In addition to AEs agregates, we also observed parts of AEs that appeared synapsed – based on their characteristic distance from each other, leading to an increase of the total number of synaptic structures in *afd1-4* (41.1±8.6). However, we never observed a central element or cytologically wild-type SCs in *afd1-4* (Fig. 4J). The maximum length of synapsed regions in *afd1-4* reached 24% of those in wild type. Furthermore, although more synapsis was detected in *afd1-4*, most of the AEs were paired non-homologously. In particular, we observed non-homologous 'self-synapsis', manifested by fold-backs of AEs on the same chromosomes (Fig. 4K,L) as well as exchanges of synaptic partners, manifested as chromosomes that pair with one partner in one region along

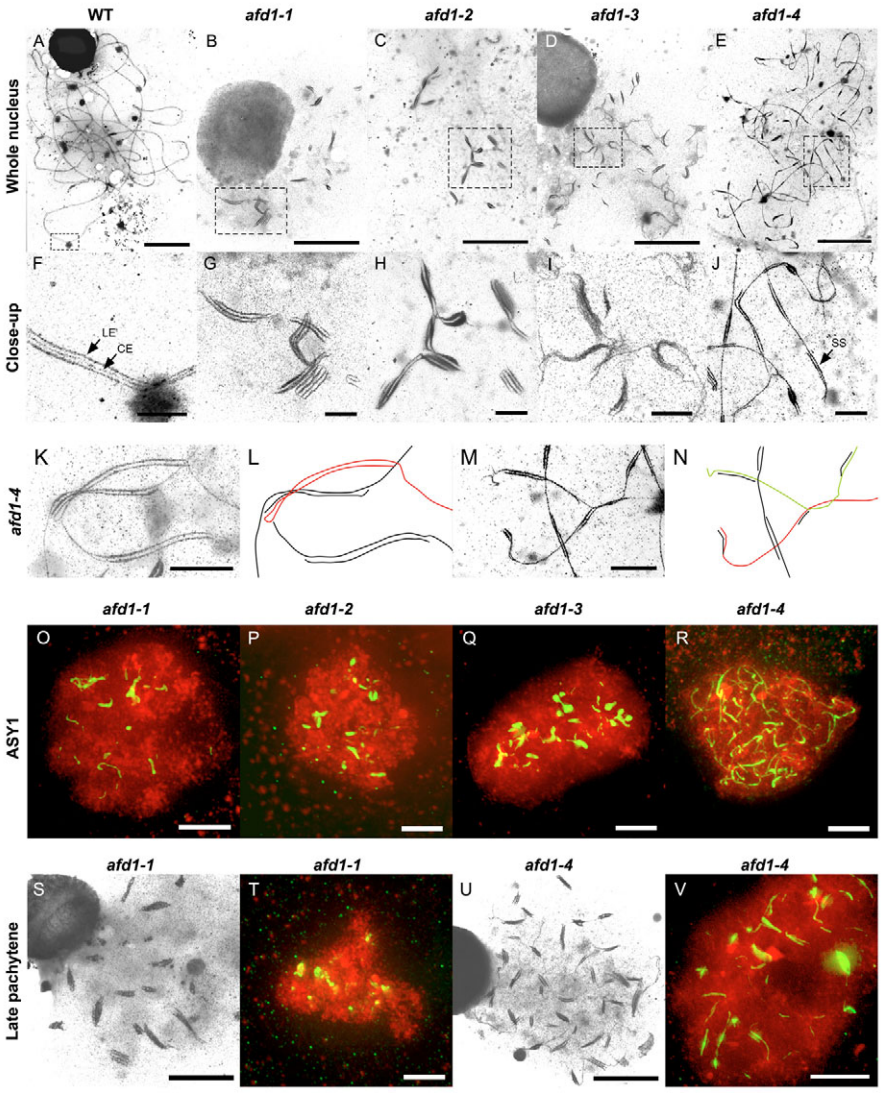

Fig. 4. AE elongation is partially rescued in the weak *afd1* alleles. (A-J) TEM analysis of synaptonemal spreads from wild-type and *afd1* meiocytes. SC in the wild type at pachytene (A) with a close-up (F) showing two lateral elements (LE) and a central element (CE). The stained round patches correspond to kinetochores, the large circle is the nucleolus. Short synaptic structures in *afd1-1* (B) during early prophase I with a close-up (G) showing their multilayered composition. Short synaptic structures in *afd1-2* (C) with a close-up (H) showing their multilayered and entangled shape. Short synaptic structures surrounded with elongated shaggy filaments in *afd1-3* (D,I). Elongated AEs in *afd1-4* with synaptic structures (SS), and regions where two axial elements are coalligned similar to normal synapsis (E,J). (K-N) Non homologous synapsis in *afd1-4* as shown by synapsis occurring within the same AE (red; K,L) and between different partners (red and green; M,N). (O-R) Localization of ASY1 in *afd1*-mutant nuclei. Patches of staining could correspond to the synaptic structures observed by TEM. Elongated AEs are clearly visible in *afd1-3* and *afd1-4*. (S-V) Synaptic structures (S,U) and ASY1/HOP1 immunostaining (T,V) in *afd1-1* and *afd1-4*, showing that AEs and ASY1/HOP1 are still present in late pachytene–early diplotene. Bars in A-E and K-V, 5 μm, in F-J, 1 μm.

its length and with a different partner in another region (Fig. 4M,N). The partial rescue of AE elongation in *afd1-4* is thus necessary but not sufficient for homologous synapsis. At late pachytene, in all the *afd1* alleles, unsynapsed AEs disappeared and only the AEs aggregates remained (Fig. 4S,U).

To confirm the presence of AE revealed by the TEM data, we performed immunostaining experiments with the antibody against ASY1/HOP1 (Armstrong et al., 2002). ASY1 is the *Arabidopsis* homolog of HOP1 and a component of the AEs (Hollingsworth et al., 1990; Smith and Roeder, 1997; Armstrong et al., 2002). ASY1/HOP1 staining closely resembled the TEM data. Although we detected an ASY1/HOP1 signal in all the *afd1* alleles, we only observed long-stretched staining of ASY1/HOP1 protein on *afd1-4* chromosomes (Fig. 4O-R). In *afd1-1* and *afd1-2*, only short protein stretches were detected (Fig. 4O,P). In *afd1-3*, we observed larger patches and lines of ASY1/HOP1 staining (Fig. 4Q). In *afd1-4*, the ASY1/HOP1 stained area was significantly more elongated than in the null-alleles (compare Fig. 4R with Fig. 4P). In late pachytene ASY1/HOP1 was present in all the *afd1* alleles as stretches and short lines (Fig. 4T,V).

Based on these data, we conclude first that AFD1 is not absolutely required for the initial recruitment of AEs and acts downstream of ASY1/HOP1. Second, AFD1 is required for AE elongation, and this function depends on the strength of the *afd1* alleles. Third, partial AE elongation alone is not sufficient to allow central element recruitment and homologous synapsis.

AFD1 is absolutely required for homologous pairing

To further address the role of AFD1 in homologous pairing, we used a 5S rRNA locus-specific FISH probe to monitor the extent of homologous pairing in the *afd1* alleles. In the wild type, at pachytene, the 5S rRNA loci are paired and appear as a single large focus per nucleus (Fig. 5A). In the four *afd1* alleles, the 5S rRNA foci were seen as two distinct spots in 100% of the *afd1-1* and *afd1-2* cells, 97% of the *afd1-3* cells, and 96% of the *afd1-4* cells and, most often, each spot was doubled because the lack of arm cohesion increased the distance between sister chromatids (Fig. 5B-D). Therefore, as previously shown for homologous synapsis, full AFD1 activity is necessary for homologous pairing. The absence of homologous pairing in all the alleles did not correlate with the variable extent of AE elongation in the *afd1* alleles. In *afd1-4* in particular, even though we observed a threefold increase in the number of synaptic structures and a dramatic increase in AE elongation, the frequency of homologous pairing was comparable to that of the null-alleles. This further confirms that the AFD1-dependent homologous pairing does not rely solely on the presence of elongated AEs. To investigate further the absence of homologous pairing in *afd1*, we analyzed two events possibly involved in the AFD1-dependent homologous pairing: telomere clustering and RAD51 localization on chromosomes.

Bouquet formation occurs in *afd1-4*

In the wild type, telomeres attach to the nuclear envelope at the leptotene-zygotene transition and form a tight bouquet at zygotene as described previously (Golubovskaya et al., 2002; Harper et al., 2004) (Fig. 5E). In *afd1-1* and *afd1-2*, telomeres remained scattered throughout the nucleus and never formed a bouquet (Fig. 5F). In *afd1-3*, telomeres could attach to the nuclear envelope, but no bouquet was visible (Fig. 5G). In *afd1-4*, telomeres attached to the nuclear envelope and the bouquet formed in 20% of the nuclei (Fig. 5H). To check whether bouquet formation requires normal AEs at chromosome ends, we performed an immunoFISH experiment in the wild-type and in the *afd1-4* allele using a telomere FISH probe and both the anti-AFD1 and anti-ASY1/HOP1 antibodies. We did not detect a stronger ASY1/HOP1 or AFD1 signal at the telomeres, showing that bouquet formation does

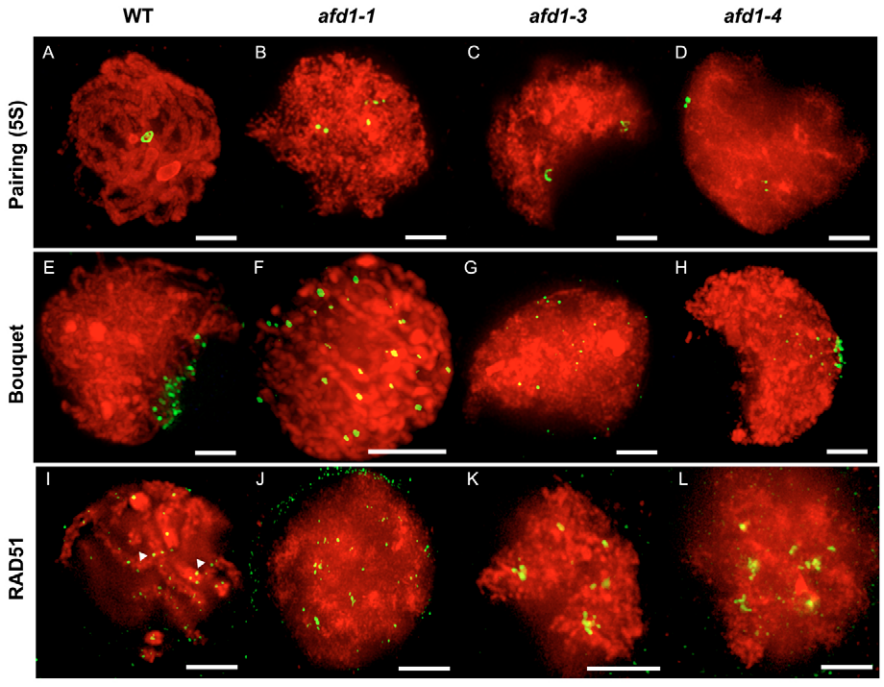

Fig. 5. Bouquet formation is rescued in *afd1-4*, but homologous pairing and RAD51 distribution are impaired in all the *afd1* alleles. (A-D) Homologous pairing in wild-type and *afd1* nuclei during pachytene using FISH with 5S rRNA probe (green) and DAPI staining (red). (A) Paired 5S rRNA focus in the wild type. (B-D) Unpaired and doubled 5S rRNA foci in *afd1-1*, *afd1-3*, *afd1-4*. (E-H) Bouquet formation in wild-type and *afd1* mutant nuclei at zygotene shown by FISH with telomere probe (green). (E) Bouquet in wild type. (F,G) Dispersed telomeres in *afd1-1* and *afd1-3* nuclei. (H) Bouquet in *afd1-4* nuclei. (I-L) RAD51 foci (green) morphology and distribution during pachytene monitored by immunofluorescence. (I) Multiple round RAD51 foci in wild-type nuclei during pachytene; some foci are paired (arrowheads). (J-L) Cluster of RAD51 foci in *afd1-1*, *afd1-3* and *afd1-4*. Bar, 5 μm.

not depend on a preferential recruitment of either AFD1 or ASY1/HOP1 at the chromosome ends, but instead depends on the recruitment of AEs on the entire chromosomes (supplementary material Fig. S3). On the basis of these data, we concluded that the rescued AE elongation in *afd1-4* could partly rescue the formation of a bouquet, but the formation of the bouquet in *afd1-4* was not able to significantly increase the frequency of homologous pairing in this allele. This suggests that bouquet formation is not a major contributor to the AFD1-dependent homologous pairing. Alternatively, it is possible that the presence of short AEs in *afd1* prevents the maintainence of the bouquet for a long enough time to facilitate pairing.

AFD1 is absolutely required for proper RAD51 distribution and polymerization

In wild-type maize, RAD51 foci form on the chromosomes at the beginning of zygotene and reach a maximum of about 500 per nucleus by mid-zygotene when chromosomes are pairing and synapsing. In zygotene, wild-type cells contain either single RAD51 foci or doubly contiguous RAD51 foci on paired chromosomes (Franklin et al., 1999). In pachytene, the RAD51 foci are brighter, often seen as two paired foci, and their number is reduced (Fig. 5I). In diplotene, no RAD51 foci are detected (Franklin et al., 1999). Mutants with defects in homologous pairing exhibit a significant decrease in the number of RAD51 foci at zygotene, corresponding to the degree of their pairing defects, suggesting that RAD51 might have a role in the homology search in addition to its known role in meiotic recombination (Franklin et al., 1999; Franklin et al., 2003; Pawlowski et al., 2003). As previously described, the number of RAD51 foci is reduced in *afd1-1* compared with that of the wild type, even at pachytene (Pawlowski et al., 2003) (Fig. 5J). Additionally, we found that the shape of the RAD51 foci in *afd1* is very different than that of the wild type. In particular, in all the *afd1* alleles, most of the RAD51 foci aggregated in bright and long patches (Fig. 5J-L). The RAD51 aggregates in *afd1-3* and *afd1-4* were particularly long, reaching a maximun of 2 μm (Fig. 5L; supplementary material Fig. S4). In comparison, in the wild type, the brightest and longest foci, which are found at pachytene, are never longer than 0.5 μm (Fig. 5I). The number of these bright RAD51 aggregates was highest in *afd1-4* (29±5), in comparison with *afd1-1*, *afd1*-2 and *afd1-3* (7±2.6, 6.8±1 and 8.8±1.6, respectively), suggesting that rescuing AE elongation in *afd1-4* facilitates the recruitment of more RAD51, but is not sufficient to form normal RAD51-foci morphology and distribution. In this respect, the number of cytologically wild-type, round RAD51 foci that were excluded from the RAD51 aggregates was extremely low (<10) in all the *afd1* alleles (Fig. 5J-L; supplementary material Fig. S4), showing that AFD1 is required for the proper morphology and distribution of RAD51 on the chromosomes.

We have cloned *afd1*, the first *rec8* homolog in maize. A new series of alleles of *afd1* allowed us to develop for the first time a unified model for chromosome behavior during meiotic prophase I in maize. By analyzing the phenotype of weak and strong alleles, we showed that, (1) AFD1 is required for AEs elongation but not AEs recruitment, (2) bouquet formation requires elongated AEs but not the installation of the recombination machinery, (3) homologous pairing relies on the formation of complete AEs and, (4) complete AEs installation is required for the appropriate deposition of the recombination machinery independently of bouquet formation. This model is summarized in a cartoon as Fig. 6.

	afd1-1	*afd1-2*	*afd1-3*	*afd1-4*
Leptotene chr. structure	–	–	+	+
Zygotene chr. structure	–	–	–	+/–
Pachytene chr. structure	–	–	–	–
AEs recruitment	+	+	+	+
AEs elongation	–	–	+/–	50%
Bouquet	–	–	–	20%
Homologous pairing	–	–	–	–
Homologous synapsis	–	–	–	–

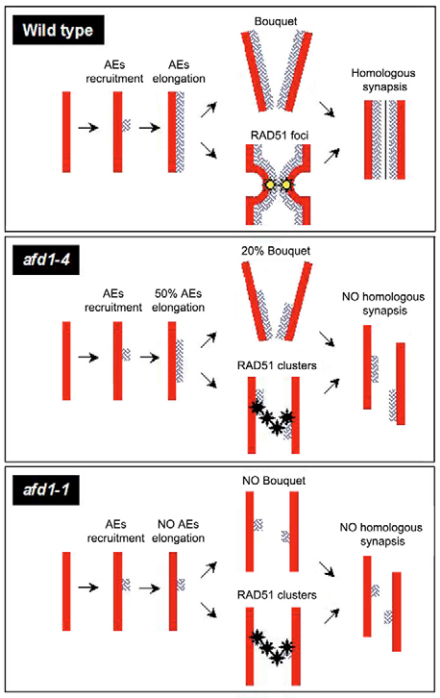

Fig. 6. Summary of *afd1* phenotypes. In the wild type, AEs are recruited and elongate along the entire chromosome. Telomere clustering requires elongated AEs. RAD51 is recruited and forms paired foci during recognition of homologous chromosomes. The bouquet, RAD51 and other unknown factors contribute to homologous pairing and synapsis. In *afd1-1*, AEs are recruited but their elongation is arrested. This impacts on both bouquet formation, RAD51 polymerization, homologous pairing and synapsis. In *afd1-4*, AEs are recruited and 50% of normal AEs elongation occurs. These AEs are sufficiently long to allow bouquet formation in 20% of the meiocytes. However, RAD51 polymerization is impaired and homologous pairing and synapsis does not occur. Therefore, homologous pairing and synapsis do not solely rely on the presence of elongated AEs and the bouquet. On the basis of these data, we propose that AFD1/REC8 controls the extent of AE elongation prior to the proper distribution of the recombination machinery, leading to pairing of homologous chromosomes independently of bouquet formation.

Discussion

In the *afd1* null-mutant, we see a series of significant defects. The first detectable defect is the absence of leptotene chromosome structure. By comparing null-alleles and weak *afd1* alleles, we found a correlation between the presence of leptotene structure, the extent of AEs elongation and the extent of AFD1 localization on chromosomes, which strongly suggests that AFD1's earliest meiotic function is to control and contribute to AEs elongation. In meiocytes fixed in 2% formaldehyde, AFD1 and ASY/HOP1 colocalized not only on axial elements but also on lateral elements, strongly suggesting that AFD1 is actually a component of axial/lateral elements.These data fit the current model that REC8 is a structural component of the synaptonemal complex (Molnar et al., 2003; Chelysheva et al., 2005).

However, we show that AFD1 has more than a structural role in AEs formation. Based on the presence of the ASY1/HOP1 signal and the AE-like structure in *afd1* null-alleles, we propose that AFD1 acts downstream of both ASY1/HOP1 and AE recruitment. The observation of longer AEs in the weaker *afd1* allele and the lack of normal SC structure in all *afd1* alleles suggests that instead of AEs recruitment, the main function of AFD1/REC8 is to control and/or contribute to AEs elongation and synapsis.

The absence of AEs elongation in the *afd1* null-alleles has a strong impact on the subsequent steps of meiotic prophase and demonstrated that AEs elongation is crucial for bouquet formation, RAD51 distribution, homologous pairing and homologous synapsis. However, using weaker *afd1* alleles, we are able for the first time to dissociate the effect of AFD1/REC8 on AEs formation from its role in bouquet formation, RAD51 distribution, homologous pairing and synapsis.

The mechanism by which the bouquet is formed is not known because very few bouquet mutants have been identified. The role of the cytoskeleton in bouquet formation is under debate, the proteins involved in forming the attachment to the nuclear envelope are not known and the role of AEs in bouquet formation has not been defined (Harper et al., 2004; Trelles-Sticken et al., 2005). In *afd1-1*, *afd1-2* and *afd1-3*, the presence of short axial elements did not lead to bouquet formation. In *afd1-4* alleles, 20% of the meiocytes had partially or completely formed bouquets, consistent with the increased levels of axial elements observed in these mutant plants. This is, to our knowledge, the first demonstration that bouquet formation depends on a threshold of AEs elongation. However, AEs elongation is most probably not sufficient for bouquet formation because in mouse *rec8* mutants bouquet formation does not occur, even though the extent of AEs elongation is comparable to that of the wild type (Xu et al., 2005).

Furthermore, the analysis of bouquet formation and RAD51 distribution in the *afd1* mutant alleles allowed us to investigate the relation between bouquet formation and recombination machinery. In *afd1-4*, distribution and morphology of the RAD51 foci were impaired even though bouquet was present, showing that bouquet formation occurs independently of RAD51 distribution. This is consistent with the observation that *spo11* mutants in yeast and *Sordaria*, which lack recombination, make normal bouquets (Storlazzi et al., 2003; Trelles-Sticken et al., 1999). Although REC8 is required for bouquet formation in maize and mouse (Xu et al., 2005), the role of REC8 in bouquet formation is not conserved in yeast. A *rec8* deletion induced a persistent telomere clustering in prophase-I-arrested cells in budding yeast, suggesting that REC8 is required for the resolution of the bouquet – rather than its formation – during zygotene in this organism (Trelles-Sticken et al., 2005). Knowing that recombination mutants also have persistent bouquets, this could be an indirect effect mediated by the requirement of REC8 to recruit the recombination machinery (Harper et al., 2004).

The relation between bouquet formation and homologous pairing is under debate. The maize mutant *pam1* is specifically impaired in the formation of a full cluster of telomeres (Golubovskaya et al., 2002). In *pam1*, homologous pairing is dramatically reduced, suggesting that bouquet formation facilitates the recognition of homologous chromosomes. Mechanistically, clustering telomeres may facilitate homologous pairing by initiating the pairing of a few loci that could allow the rest of the chromosome to zip-up mechanically (Bass et al., 1997; Harper et al., 2004). Here, we showed on the contrary that, the presence of a bouquet in *afd1-4* is not sufficient to promote homologous pairing of the 5S rRNA locus, a sequence near the telomeres. Absence of pairing is therefore most probably due to the greatly reduced number of recombination inititation events in the *afd1* mutants, rather than a direct effect of the bouquet. In contrast to wild-type nuclei, *afd1-1* nuclei are not stained by the TUNEL assay suggesting that meiosis-specific DNA damage, i.e. double-strand breaks, are not made in the *afd1* null-allele (data not shown). Altogether these data suggest that the role of REC8 in bouquet formation is independent from its role in homologous pairing.

Although we could uncouple AEs elongation and bouquet formation from homologous pairing, we were not able to dissociate defects in homologous pairing from defects in RAD51 distribution and polymerization in any of the *afd1* alleles. It is therefore possible that the role of AFD1 in homologous pairing relies on the recombination machinery in addition to the AEs. Based on previous work in maize, RAD51 is thought to participate in recognizing homologous chromosomes prior to homologous synapsis (Franklin et al., 1999; Franklin et al., 2003; Pawlowski et al., 2003; Pawlowski et al., 2004). Thanks to the large meiotic chromosomes in maize, we were able to observe the morphology of RAD51 foci with high resolution in the *afd1* alleles. Morphology of RAD51 foci in *afd1* was similar, although the foci number was higher compared with that in maize *phs1*, *dsyCS* and *segII* mutants, which are also impaired in recognizing homologous chromosomes and homologous synapsis (Pawlowski et al., 2003; Pawlowski et al., 2004) (I.N.G., unpublished data). The RAD51 clusters in these mutants have been proposed to be a manifestation of failure in the search for chromosomal homology (Pawlowski et al., 2003; Franklin et al., 2003; Pawlowski et al., 2004). Based on these observations, the role of AFD1 in recruiting and controlling the distribution of the recombination machinery might contribute, directly or indirectly, to the recognition of homologous chromosomes.

The *absence of first division 1* mutant originally received its name because of the presence of an equational first division due to a complete lack of sister chromatid cohesion (SCC) (Golubovskaya and Mashnenkov, 1975). This mutant has been used in further studies to explore the link between SCC and histone phosphorylation (Kaszas and Cande, 2000), and

RAD51 and ZmSGO1 recruitment (Pawlowski et al., 2003; Hamant et al., 2005). This work is the first description of AFD1 as a REC8 homolog in maize, and confirms the role of REC8 in SCC and kinetochore orientation in maize. We have shown previously that ZmSGO1 maintains centromeric cohesion at the end of MI, and that ZmSGO1 recruitment is impaired in *afd1-1* (Hamant et al., 2005). Defects in centromeric cohesion in the *afd1* mutants are thus probably the result of the loss of both AFD1 and ZmSGO1 at the centromere. Interestingly, fission yeast *rec8* mutants also display an equational first division. The characterization of the MOA1 protein has recently allowed the dissection of the functions of REC8 at the centromeres (Yokobayashi and Watanabe, 2005), providing a complementary analysis to our study focused on events in prophase I.

In summary, the characterization of a series of *afd1* alleles has unraveled the role of AFD1/REC8 in controlling AEs elongation and the formation of lateral elements. It allowed us to monitor the impact of the extent of AEs elongation on bouquet formation and has demonstrated that, AFD1-dependent homologous pairing requires full elongation of AEs and is associated with the proper distribution of the recombination machinery but does not rely on bouquet. We believe that allelic series of *rec8* in other organisms would provide new information on the role of REC8 in the coordination of prophase I events and might help us to understand the differences between yeast, *C. elegans*, *Arabidopsis* and mammalian *rec8* mutant phenotypes, and to dissect the functions of REC8 that are conserved throughout species.

Materials and Methods

Plant material

The recessive *afd1-1* reference allele was originally induced with N-nitroso-N-methylurea in the W23 inbred in 1974 (Golubovskaya and Mashnenkov, 1975). The *afd1-2* came from a directed *Mutator (Mu)*-tagging experiment of the maize leaf gene *tiedyed1* (*tdy1*), which is tightly linked with *afd1-1*. The TUSC procedure (Meeley and Briggs, 1995; Chuck et al., 1998) was used to isolate the *afd1-3* and *afd1-4* lines by reverse genetics.

Genetics

Previously, two mutations (*afd1-1* and *tiedyed1*) had been mapped at the distal region of the long arm of chromosome 6 with a basic set of B-A translocations. To estimate the linkage between the two genes, heterozygous plants for *afd1-1* reference allele were crossed with homozygous *tdy1/tdy1* plants. We only considered the F2 progeny that segregated the *afd1* phenotype. Of 1000 F2 progeny, we never obtained an *afd1-tdy1* double mutant but we did obtain three segregating phenotypes: green-fertile, green-sterile and tiedyed-fertile in a ratio 2:1:1, showing that the two genes are closely linked. A fine-mapping of the *afd1* gene was conducted. For simple sequence repeats (SSRs) segregation analysis, the *afd1-1* heterozygotes (W23) were out crossed onto the Mo17 and B73 inbred lines and self-pollinated. Polymorphisms between W23 and Mo17 inbred lines were identified for chromosome 6 SSR umc 2059 and bngl 1136 markers, both located on bin 6.08. A total of 48 *afd1-1* mutants from segregated F2 families were used to fine-map the gene. The PCR samples were separated by electrophoresis on a 4.5% Apex agarose/TAE gel and stained with ethidium bromide to visualize bands. The chromosomal position of *afd1* was also confirmed by in situ hybridization (Wang et al., 2006). To demonstrate allelism between the four mutant lines (*afd1-1*, *afd1-2*, *afd1-3*, *afd1-4*), heterozygotes for all alleles were crossed with each other, and F1 progenies were tested for segregation of sterility. F1 of all combination-segregated one-fourth of sterile plants and three-quarters of fertile plants. Cytological analysis showed that F1 *afd1-2/afd1-1* displayed the same phenotype as *afd1-1*. Heterozygotes *afd1-1/+* and hemizygotes for the deletion allele *afd1-2/+* displayed a wild-type phenotype.

Primers

RT-PCR and RACE-PCR primers used to amplify *afd1* were: OH-16 (5′-ATG-GCGGCGACGCTCCACTCGAAGATC-3′), OH-27 (5′-TCTCGTACACGATCA-CCACGCCACC-3′), OH-57 (5′-GATCTTCGAGTGGAGCGTCGCCGCCAT-3′), OH-62 (5′-ACAGTGACCATAGTGTTACTCCTGGAAGT-3′), OH-61 (5′-GAC-TTCCAGGAGTAACACTATGGTCACTGT-3′), OH-80 (5′-TTCAGTAAGTGC-TTTCAGGACAACTTAGTT-3′), OH-91 (5′-AAGAGACAAGTAGACAACCCA-GCTCT-3′). RT-PCR primers used to amplify a partial *smc3* cDNA were: OH-33 (5′-GAAGCAAAGGGGGTCACTTGAGAAAGC-3′), OH-36 (5′-TTCACGGAA-GTGCCTTGCAACCCCTTT-3′).

PCR Amplification of *afd1* genomic sequence

Genomic DNA was isolated from secondary ears and leaves from the wild-type, and homozygotes of four *afd1* alleles using a CTAB-based protocol (Doyle and Doyle, 1990). DNA (1 μg) was used as a template in a 25 μL reaction. PCR amplification was performed with the Taq polymerase Roche kit (Roche Diagnostics, IN). PCR cycles were as follows: ten cycles of 30 seconds at 94°C, 30 seconds at 65°C (–1°C/cycle), 1.5 minutes at 72°C, followed by 35 cycles of 30 seconds at 94°C, 30 seconds at 55°C, and 1.5 minutes at 72°C, followed by 5 minutes at 72°C and were performed in a GeneAmp PCR system 2400 (PerkinElmer, Wellesley, MA). Amplified fragments were cloned in pCR2.1 (Invitrogen, Carlsbad, CA) and sequenced in both directions.

RT- and RACE-PCR

Total RNA from A344 tissue-roots (1 cm from the tip), 7-day-old leaves, 3-week-old leaves, young tassel- and ear-containing meiocytes, and old tassel-containing pollen – was isolated following the Trizol reagent protocol (Gibco-BRL). RNA was also isolated from tassel-containing meiocytes from homozygotes of the four *afd1* alleles following the same protocol. 2 μg of each RNA sample were run on a 1.2% agarose gel and the intensities of rRNA bands were compared to assess the amount of RNA template. These RNAs were subjected to reverse transcription using the MMLV reverse transcriptase kit (Promega, Madison, WI). PCR amplification was then performed with 5 μl of the reverse transcription sample. Primers OH-33 and OH-36, which are specific for the maize *smc3* gene, were used as an internal control and confirmed that an equal amount of amplifiable cDNA was available in all the samples. Primers OH-16 and OH-61 were used to amplify part of the *afd1* cDNA (exon 2 to exon 15). RACE samples were prepared with the RFLM-RACE Kit (Ambion, Austin, TX) according to the manufacturer's instructions. The 5′ RACE primers were OH-27 and OH-57 and the 3′ RACE primer was OH-62. Continuity of the *afd1* cDNA was checked by PCR with primers OH-91 and OH-80. RT-PCR and RACE-PCR products were resolved, cloned and sequenced as described above.

Cytology

A smear acetocarmine technique was used to investigate chromosome segregation in *afd1* and to confirm the *afd1* mutant phenotype in plants from *afd1* families that segregated a male sterile phenotype. Immature tassels were fixed in Farmer's fixative (95% ethanol and glacial acetic acid at the ratio of 3:1) and stained with 2% acetocarmine, squashed, and observed with a light-microscope (Golubovskaya et al., 1993).

For FISH, immunostaining and immunoFISH, most anthers from pre-emerged tassels were fixed with 4% formaldehyde in buffer A and stored as described in Golubovskaya et al. (Golubovskaya et al., 2002); for immunostaining experiments, remaining anthers were fixed with 2% formaldehyde, as mentioned in the text. Meiocytes were embedded in polyacrylamide as described in Hamant et al. (Hamant et al., 2005). Staging criteria were as described previously (Dawe et al., 1994; Bass et al., 1997; Golubovskaya et al., 2002). FISH was performed as described in Golubovskaya et al. (Golubovskaya et al., 2002). Results on figures are representative of at least 25 meiocytes for each stage.

To generate anti-AFD1 antibody, we cloned a partial *afd1* cDNA corresponding to amino acids 227-462 of the AFD1 protein (a region that was successfully used to raise the SYN1/AtREC8 antibody in *Arabidopsis*) into the pGEX-4T-3 plasmid in translational fusion with GST. The protein was expressed in *E. coli* BL21 and purified with the GST purification kit (Amersham Biosciences, Piscataway, NJ). The AFD1 antibody was then raised in rats (Strategic Biosolutions, Newark, DE). No staining on the chromosomes was obtained with the pre-immune antiserum in the wild-type or the AFD1 antibody in the *afd1-2* null-allele.

Immunostaining was performed as described by Pawlowski et al. (Pawlowski et al., 2003) with the following modifications: 4% BSA (no donkey serum) was used to block the samples, antibodies were not pre-cleared (except anti-RAD51) and secondary antibodies were incubated for 1 hour and washed three times only. In addition to the anti-AFD1 antibody, we used the anti-ZmSGO1 antibody (1:50) (Hamant et al., 2005), anti-RAD51 antibody (1:200) (Franklin et al., 1999; Pawlowski et al., 2003; Franklin et al., 2003), an anti-ASY1 antibody (1:50), kindly provided by C. Franklin (University of Birmingham, UK) (Armstrong et al., 2002) and a SYN1 antibody (1:50), kindly provided by C. Makaroff (Miami University, Oxford, OH) (Cai et al., 2003). We used Cy3-conjugated $F(ab')_2$ donkey anti-rat IgG and FITC-conjugated $F(ab')_2$ donkey anti-rabbit IgG secondary antibodies (1:50; Jackson ImmunoResearch, West Grove, PA). 3D-stacks of images were collected and analyzed as described by Golubovskaya et al. (Golubovskaya et al., 2002). Results on figures are representative of at least 25 meiocytes for each stage.

The ImmunoFISH protocol was adapted from Kaszas and Cande, (Kaszas and Cande, 2000). On day 1, we followed the FISH protocol (Golubovskaya et al., 2002)

and hybridized the probe overnight. On day 2, we washed the pads once with 1× SSC with 1× PBS (15 minutes); once with 1× PBS with 0.1% Tween 20 (15 minutes), followed by the immunostaining protocol (see above) with the following modifications: both the primary and secondary antibodies were incubated for 1 hour only and washed three times.

We used transmission electron microscopy to study the extent of synapsis in the *afd1* alleles in chromosome spreads of male meiocyte nuclei. The spreads were treated with silver nitrate, which stains the AEs present at leptotene and early zygotene that later become the lateral elements of the SC, after the SC is formed between paired chromosomes at pachytene. SC spreads from 24 *afd1-1*, 29 *afd1-2*, 25 *afd1-3*, 30 *afd1-4* mutant meiocytes were prepared and analyzed as described in detail by Golubovskaya et al. (Golubovskaya et al., 2002). Length of the synaptic structures was measured with softworx (Applied Precision, WA, USA).

New materials described in this publication are available for non-commercial research purposes upon acceptance and signing of a material-transfer agreement.

We thank Chris Makaroff for providing the SYN1 antiserum and Chris Franklin for providing the ASY1 antibody. We thank Meredith Sagolla for help with microscopes, and Lisa Harper, Wojciech Pawlowski, Ray Chan and David Mets for discussions and critical reading of the manuscript. We thank Barbara Rotz and her staff for excellent care of plants in the field and greenhouses. Part of this project was made possible through the use of technology developed by Pioneer Hi-Bred International, Inc. This research was supported by grants from the National Institutes of Health GM 048547, and the USDA 2003-35301-13152 to W.Z.C.

References

Armstrong, S. J., Caryl, A. P., Jones, G. H. and Franklin, F. C. (2002). Asy1, a protein required for meiotic chromosome synapsis, localizes to axis-associated chromatin in *Arabidopsis* and *Brassica*. *J. Cell Sci.* **115**, 3645-3655.

Bai, X., Peirson, B. N., Dong, F., Xue, C. and Makaroff, C. A. (1999). Isolation and characterization of *SYN1*, a *RAD21*-like gene essential for meiosis in *Arabidopsis*. *Plant Cell* **11**, 417-430.

Bass, H. W., Marshall, W. F., Sedat, J. W., Agard, D. A. and Cande, W. Z. (1997). Telomeres cluster de novo before the initiation of synapsis: a three-dimensional spatial analysis of telomere positions before and during meiotic prophase. *J. Cell Biol.* **137**, 5-18.

Bhatt, A. M., Lister, C., Page, T., Fransz, P., Findlay, K., Jones, G. H., Dickinson, H. G. and Dean, C. (1999). The *DIF1* gene of *Arabidopsis* is required for meiotic chromosome segregation and belongs to the *REC8/RAD21* cohesin gene family. *Plant J.* **19**, 463-472.

Cai, X., Dong, F., Edelmann, R. E. and Makaroff, C. A. (2003). The *Arabidopsis* SYN1 cohesin protein is required for sister chromatid arm cohesion and homologous chromosome pairing. *J. Cell Sci.* **116**, 2999-3007.

Chelysheva, L., Diallo, S., Vezon, D., Gendrot, G., Vrielynck, N., Belcram, K., Rocques, N., Marquez-Lema, A., Bhatt, A. M., Horlow, C. et al. (2005). AtREC8 and AtSCC3 are essential to the monopolar orientation of the kinetochores during meiosis. *J. Cell Sci.* **118**, 4621-4632.

Chuck, G., Meeley, R. B. and Hake, S. (1998). The control of maize spikelet meristem fate by the *APETALA2*-like gene *indeterminate spikelet1*. *Genes Dev.* **12**, 1145-1154.

Dawe, R. K., Sedat, J. W., Agard, D. A. and Cande, W. Z. (1994). Meiotic chromosome pairing in maize is associated with a novel chromatin organization. *Cell* **76**, 901-912.

Doyle, J. J. and Doyle, J. L. (1990). Isolation of plant DNA from fresh tissue. *Focus* **12**, 13-15.

Franklin, A. E., McElver, J., Sunjevaric, I., Rothstein, R., Bowen, B. and Cande, W. Z. (1999). Three-dimensional microscopy of the Rad51 recombination protein during meiotic prophase. *Plant Cell* **11**, 809-824.

Franklin, A. E., Golubovskaya, I. N., Bass, H. W. and Cande, W. Z. (2003). Improper chromosome synapsis is associated with elongated RAD51 structures in the maize *desynaptic2* mutant. *Chromosoma* **112**, 17-25.

Golubovskaya, I. N. and Mashnenkov, A. S. (1975). Genetic control of meiosis. I. Meiotic mutation in corn (*Zea mays L.*) *afd*, causing the elimination of the first meiotic division. *Genetika* **11**, 810-816.

Golubovskaya, I., Grebennikova, Z. K., Avalkina, N. A. and Sheridan, W. F. (1993). The role of the *ameiotic1* gene in the initiation of meiosis and in subsequent meiotic events in maize. *Genetics* **135**, 1151-1166.

Golubovskaya, I. N., Harper, L. C., Pawlowski, W. P., Schichnes, D. and Cande, W. Z. (2002). The *pam1* gene is required for meiotic bouquet formation and efficient homologous synapsis in maize (*Zea mays L.*). *Genetics* **162**, 1979-1993.

Hamant, O., Golubovskaya, I., Meeley, R., Fiume, E., Timofejeva, L., Schleiffer, A., Nasmyth, K. and Cande, W. Z. (2005). A REC8-dependent plant Shugoshin is required for maintenance of centromeric cohesion during meiosis and has no mitotic functions. *Curr. Biol.* **15**, 948-954.

Harper, L., Golubovskaya, I. and Cande, W. Z. (2004). A bouquet of chromosomes. *J. Cell Sci.* **117**, 4025-4032.

Hollingsworth, N. M., Goetsch, L. and Byers, B. (1990). The *HOP1* gene encodes a meiosis-specific component of yeast chromosomes. *Cell* **61**, 73-84.

Kaszas, E. and Cande, W. Z. (2000). Phosphorylation of histone H3 is correlated with changes in the maintenance of sister chromatids cohesion during meiosis in maize, rather than the condensation of the chromatin. *J. Cell Sci.* **113**, 3217-3226.

Kitajima, T. S., Miyazaki, Y., Yamamoto, M. and Watanabe, Y. (2003). Rec8 cleavage by separase is required for meiotic nuclear divisions in fission yeast. *EMBO J.* **22**, 5643-5653.

Klein, F., Mahr, P., Galova, M., Buonomo, S. B. C., Michaelis, C., Nairz, K. and Nasmyth, K. (1999). A central role for cohesins in sister chromatid cohesion, formation of axial elements, and recombination during yeast meiosis. *Cell* **98**, 91-103.

Lee, J. Y. and Orr-Weaver, T. L. (2001). The molecular basis of sister-chromatid cohesion. *Annu. Rev. Cell Dev. Biol.* **17**, 753-777.

Lin, Y., Larson, K., Doer, R. and Smith, G. (1992). Meiotically induced *rec7* and *rec8* genes of *Schizosaccharomyces pombe*. *Genetics* **132**, 75-85.

Meeley, B. and Briggs, S. P. (1995). Reverse genetics for maize. *Maize Newsletter* **69**, 67-82.

Molnar, M., Baehler, J., Sipiczki, M. and Kohli, M. (1995). The *rec8* gene of *Schizosaccharomyces pombe* is involved in linear element formation, chromosome pairing and sister-chromatid cohesion during meiosis. *Genetics* **141**, 61-73.

Molnar, M., Doll, E., Yamamoto, A., Hiraoka, Y. and Kohli, J. (2003). Linear element formation and their role in meiotic sister chromatid cohesion and chromosome pairing. *J. Cell Sci.* **116**, 1719-1731.

Nasmyth, K. (1999). Separating sister chromatids. *Trends Biochem. Sci.* **24**, 98-104.

Nonomura, K., Nakano, M., Eiguchi, M., Suzuki, T. and Kurata, N. (2006). PAIR2 is essential for homologous chromosome synapsis in rice meiosis I. *J. Cell Sci.* **119**, 217-225.

Page, S. L. and Hawley, R. S. (2003). Chromosome choreography: the meiotic ballet. *Science* **301**, 785-789.

Pasierbek, P., Jantsch, M., Melcher, M., Schleiffer, A., Schweizer, D. and Loidl, J. (2001). A *Caenorhabditis elegans* cohesion protein with functions in meiotic chromosome pairing and disjunction. *Genes Dev.* **15**, 1349-1360.

Pawlowski, W. P., Golubovskaya, I. N. and Cande, W. Z. (2003). Altered nuclear distribution of recombination protein RAD51 in maize mutants suggests the involvement of RAD51 in meiotic homology recognition. *Plant Cell* **15**, 1807-1816.

Pawlowski, W. P., Golubovskaya, I. N., Timofejeva, L., Meeley, R. B., Sheridan, W. F. and Cande, W. Z. (2004). Coordination of meiotic recombination, pairing, and synapsis by PHS1. *Science* **303**, 89-92.

Schleiffer, A., Kaitna, S., Maurer-Stroh, S., Glotzer, M., Nasmyth, K. and Eisenhaber, F. (2003). Kleisins–a superfamily of bacterial and eukaryotic SMC protein partners. *Mol. Cell* **11**, 571-575.

Smith, A. V. and Roeder, G. S. (1997). The yeast Red1 protein localizes to the cores of meiotic chromosomes. *J. Cell Biol.* **136**, 957-967.

Stoop-Myer, C. and Amon, A. (1999). Meiosis: Rec8 is the reason for cohesion. *Nat. Cell Biol.* **1**, E125-E127.

Storlazzi, A., Tesse, S., Gargano, S., James, F., Kleckner, N. and Zickler, D. (2003). Meiotic double-strand breaks at the interface of chromosome movement, chromosome remodeling, and reductional division. *Genes Dev.* **17**, 2675-2687.

Trelles-Sticken, E., Loidle, J. and Scherthan, H. (1999). Bouquet formation in budding yeast: initiation of recombination is not required for meiotic telomere clustering. *J. Cell Sci.* **112**, 651-658.

Trelles-Sticken, E., Adelfalk, C., Loidl, J. and Scherthan, H. (2005). Meiotic telomere clustering requires actin for its formation and cohesin for its resolution. *J. Cell Biol.* **170**, 213-223.

Uhlmann, F. (2003). Chromosome cohesion and separation: from men and molecules. *Curr. Biol.* **13**, R104-R114.

Wang, C.-J. R., Harper, L. and Cande, W. Z. (2006). High-resolution single-copy gene fluorescence in situ hybridization and its use in the construction of a cytogenetic map of maize chromosome 9. *Plant Cell* **18**, 529-544.

Watanabe, Y. and Nurse, P. (1999). Cohesin Rec8 is required for reductional chromosome segregation at meiosis. *Nature* **400**, 461-464.

Xu, H., Beasley, M. D., Warren, W. D., van der Horst, G. T. and McKay, M. J. (2005). Absence of mouse REC8 cohesin promotes synapsis of sister chromatids in meiosis. *Dev. Cell* **8**, 949-961.

Yokobayashi, S. and Watanabe, Y. (2005). The kinetochore protein Moa1 enables cohesion-mediated monopolar attachment at meiosis I. *Cell* **123**, 803-817.